Article

Characterizing a Silver Nanoparticle-Based Electrochemical Biosensor for Shiga Toxin Detection

Dhruv Patel,* Madison Hansen, Christopher Lambert, Shruti Hegde, Harikrishnan Jayamohan, Bruce K. Gale, and Himanshu Jayant Sant
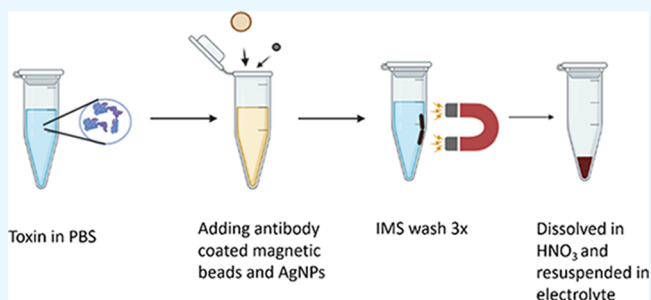
Cite This: ACS Omega 2023, 8, 40898−40903

Read Online

ACCESS | Metrics & More | Article Recommendations | Supporting Information

ABSTRACT: Shiga toxins (1, 2) regularly cause outbreaks and food recalls and pose a significant health risk to the infected population. Therefore, new reliable tools are needed to rapidly detect Shiga toxin cost-effectively in food, water, and wastewater before human consumption. Enzyme immunoassay and polymerase chain reaction approaches are the gold standard detection methods for the Shiga toxin. However, these methods require expensive instruments along with expensive reagents, which makes them hard to convert into point-of-use and low-cost systems. This study introduces an electrochemical biosensing method that utilizes silver nanoparticles (AgNPs) as electrochemical tags and commercially available low-cost screen-printed carbon electrodes for detection. This study introduces the modification of reference electrodes on commercially available screen-printed carbon electrodes to detect AgNPs dissolved in nitric acid. This biosensor achieved a 2 ng/mL lowest measured concentration for Shiga toxin-1 in less than 3 h. These biosensor results also showed that the AgNP-based sensor has better linearity (for graph between peak current vs concentration) and lower standard deviation compared to gold nanoparticles (AuNP)-based electrochemical biosensors.

Toxin in PBS   Adding antibody coated magnetic beads and AgNPs   IMS wash 3x   Dissolved in HNO₃ and resuspended in electrolyte

INTRODUCTION

The economic and health cost of Shiga toxin poisoning in humans is significant,[1−3] and it is becoming an ever-increasing challenge lately.[4,5] For example, a 2017 Centers for Disease Control and Prevention report suggests that incidences of Shiga toxin-producing *Escherichia coli* (STEC) infection per 100,000 population reported to Laboratory-based Enteric Disease Surveillance increased by 132 % from 1997 to 2017.[6] The estimated economic cost of STEC infections is greater than $400 million annually.[7,8] Shiga toxins damage endothelial cells in the kidney and brain, causing renal failure and neurological complications.[9−11] Shiga toxin has more hospitalizations per infection than other foodborne illnesses caused by *Salmonella* or *Campylobacter*.[12]

The need for a reliable and sensitive detection method for Shiga toxin stems from its infectious dosage in humans and animals. A microgram quantity of Shiga toxin can be lethal and cause kidney failure, neurological complications, as well as necrosis of tissues.[13] Yutsudo et al. estimated that 63.7 μg is a lethal amount for a 45.5 kg human for Shiga toxin-1.[14] Similarly, Tesh and Eiklid and Olsnes calculated LD_{50} in mice equal to 20 and 450 μg/kg, respectively,[15,16] making Shiga toxin very dangerous.

Shiga toxin is a protein toxin included in the AB_5 holotoxins. Each holotoxin comprises a single A subunit noncovalently bound to 5 identical B subunits.[17] The B subunit binds to lipids on the surface of the cell. It brings the holotoxin inside the cytoplasm of a cell, where the A subunit catalytically activates its A1 subunit, which stops protein synthesis.[18−20] One A1 domain is enough to kill a cell. The mass of the B subunit is 7.7 kDa, whereas the mass of the A subunit is 33 kDa. The two most common Shiga toxins are Shiga toxin-1 and Shiga toxin-2.[21−23] Both have different effects on different cell types but induce apoptosis in different cell types.

Shiga toxin infection symptoms range from diarrhea to hemorrhagic colitis with chances of developing hemolytic uremic syndrome.[24−27] Additionally, there is no practical way to treat Shiga toxin poisoning.[28−30] Some antibodies induce the replication of phases, so antibody treatment is also not recommended for poisoning.[28−30] Due to the lack of available treatments, detecting Shiga toxin before its consumption or spreading as a preventive measure is necessary. Hence, rapid, point-of-use, low-cost, and reliable detection of Shiga toxin-1 is essential as a preventive tool. Detecting toxins in food or wastewater is better to avoid disasters since treatment is highly

challenging. Currently, enzyme immunoassay (EIA) and polymerase chain reaction (PCR) approaches are the gold standard detection methods for Shiga toxin.[31] However, these methods and relative works (like self-powered temperature sensors with Seebeck effect transduction for photo thermal-thermoelectric coupled immunoassay[32]) require expensive instruments and reagents, making these methods hard to convert into point-of-use and low-cost systems.

By comparison, electrochemical biosensors are easily translated to point-of-use systems.[33−35] This study uses an electrochemical detection method using silver nanoparticles (AgNPs) and low-cost, readily available screen-printed carbon electrodes (SPCEs) to detect Shiga toxin-1.

The use of AgNPs has several benefits in meeting the mentioned need for the detection of Shiga toxin-1. First, a 60 nm AgNP has 6.6 million atoms, and 100 % dissolution and stripping in 1 s would create a signal of 1 pA (calculated based on silver particle density and electron charge), which modern instruments can measure (see the Supporting Information for complete calculation). Hence, the detection of one toxin molecule connected to an AgNP in an ideal system with currently available technology would theoretically be possible. The main limitation of the system would likely be related to antibody binding efficiency.[35] Also, the science/technology behind the attachment of antibodies to AgNP is improving rapidly.[36,37] This improvement is driven by developments involving gold nanoparticle (AuNP) modification with anti-bodies,[38−40] but AgNP modification uses similar chemistry as is applied to the AuNPs.[41,42,43]

Additionally, the advantages of using AgNP-based electro-chemical biosensors, specifically over AuNP-based electro-chemical biosensors, are described as follows. First, for the yes/no test (a test that only indicates results as positive or negative instead of concentration), the current protocol could modify the current setup, requiring just a fixed voltage battery with nitric acid (HNO_3) for point-of-use detection in remote areas for possible use in the future. Second, AgNPs are 90 times cheaper than AuNPs, which are often used for biosensors. The electrochemical dissolution of nanoparticles also determines their electrochemical efficiency, and AgNPs are easier to dissolve and modify than AuNPs.[44] The most significant limitation of AgNPs is stability when the particles are coated with citrate compared to AuNPs.[44,45] That is why during the modification of AgNPs, they should be carefully stored in opaque containers. However, this can be avoided by using aluminum foil-coated tubes during antibody modification. After antibody modification, AgNPs become stable under normal light conditions (initial observation, data are not shown).

Due to the relatively low-cost and well-established protocols, an AgNPs-based biosensor is proposed for use in this study. Previous researchers have used AgNPs for biosensing applications. However, none of them used screen-printed carbon electrodes (SPCEs) to detect dissolved silver, as it requires the addition of HNO_3 in a buffer. HNO_3 reacts with the reference electrode of SPCE, which would give a higher and more variable silver detection signal. This problem is solved by treating the reference electrode with bleach, which makes exposed silver into silver chloride. Due to the extremely low K_{sp} (silver chloride (AgCl) solubility constant in water and nitric acid), Ag^+ will not form and does not contribute to the background signal. The innovation of this article is using

AgNP-based electrochemical detection with commercially available SPCE for AgNP detection.

In summary, this article describes the modification and characterization of commercially available SPCE for silver detection, selecting the best pair of antibodies for Shiga toxin detection and immunomagnetic separation (IMS)-based detection of Shiga toxin using AgNPs, and compares these results with those of our previously developed AuNP-based Shiga toxin detection approach (Figure 1).
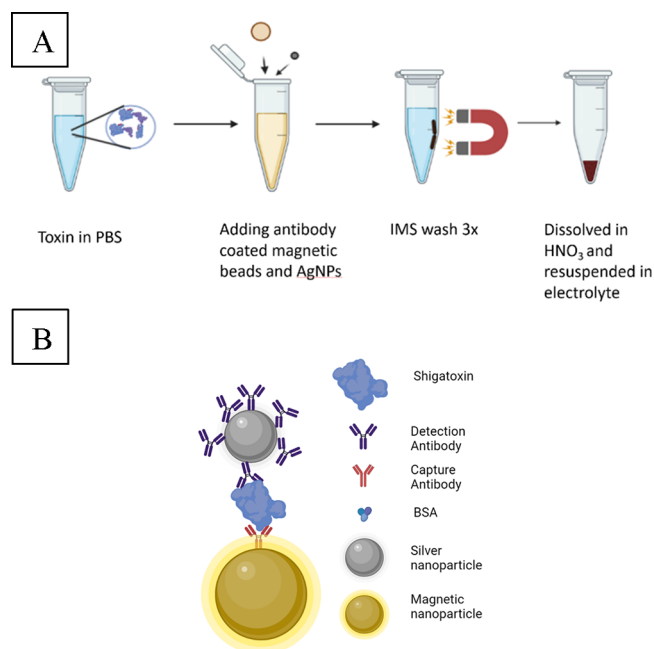

Figure 1. (A) Schematic diagram showing the protocol for the IMS-based AgNP assay, showing the toxin incubated with antibody-coated magnetic beads and silver particles. After this, the complex forms (magnetic beads-antigen-AgNPs) are washed by a standard IMS protocol. Finally, the remaining solution is dissolved and resuspended in an electrolyte. (B) Completed sandwich immunoassay. The figure is not up to the scale. Figure is made using biorender.com.

■ MATERIALS AND METHODS

Bioreagents. Shiga toxin-1 from *E. coli* (#161, List Laboratories, Campbell, CA, USA), anti-Shiga toxin-1 (rabbit), lgG (#761L, List Laboratories, Campbell, CA, USA) (described as R-antibodies), anti-Shiga toxin, camelid anti-body, and VHH (#761L, List Laboratories, Campbell, CA, USA) (described as Vh-antibodies).

Chemical Reagents. PBS buffer (# 806552, Sigma-Aldrich, MO, USA), mass spectroscopy grade water (# 900682, Sigma-Aldrich, MO, USA), acetonitrile (Catalog # 34998, from Sigma-Aldrich, Burlington, MA, USA); DSP (dithiobis(succinimidyl propionate)) (Catalog # 22585, from ThermoFisher Scientific, Cleveland, OH, USA); 3-mercapto-propionic acid (MPA), 99 % (catalog # A13261, from Alfa Aesar, Ward Hill, MA, USA); 60 nm unconjugated silver sols (catalog # 807036, from Sigma-Aldrich, Burlington, MA, USA); 20 nm unconjugated AuNPs (catalog #EM.GC20/4Pierce, from BBI Solutions Portland, ME, USA); 20X borate buffer (catalog #28341, from ThermoFisher Scientific, Cleveland, OH, USA); nitric acid, 99.999 % trace metals basis (catalog # 225711, from Sigma-Aldrich, Burlington, MA,

USA); Dynabeads MyOne carboxylic acid Invitrogen (catalog # 65012, Lot # 01188483, from ThermoFisher Scientific, Cleveland, OH, USA); Pierce EDC, no-weigh form (catalog # A35391, Lot # WL333565, from ThermoFisher Scientific, Cleveland, OH, USA); and SPCE (catalog# TE100, from CH instrument, Inc., Austin, TX, USA)

Antibody Conjugation to 60 nm AgNPs. 960 μL portion of AgNPs (60 nm, 0.02 mg/mL) was mixed with 40 μL of 2 mM borate buffer to adjust the pH to 8.5. After that, the AgNPs were modified with 10 μL of (multimonolayer) MML solution. MML solution contains 1.0 mM DSP and 10 mM MPA in acetonitrile. The solution was rotated for 2 h in rotating plates. Antibodies were attached to MML-modified AgNPs by adding 5.0 μg of the desired antibodies and mixed on a rotating plate for 3 more hours. Next, the solution was added to 100 μL of 10 % (v/v) bovine serum albumin (BSA) in 2 mM borate buffer and rotated for 6 − 8 h. Finally, AgNPs were washed with centrifugation at 2500 g for 12 min, removing the supernatant, and resuspending the AgNP pellet into 1 mL of 1 % (v/v) BSA in 2 mM borate buffer. Dynamic light scattering data are shown in Figure S3. The conjugation of AuNP-antibody is similar to that of AgNP-antibody. Please refer to our previous publication for a detailed description of this protocol.[47]

Antibody Conjugation to Magnetic Beads. The magnetic beads were modified with antibodies following instructions from the Dynabeads_MyOne (Catalog # 65012) manual from ThermoFisher.[48] In summary, 1 mL of magnetic beads was concentrated on the side wall of a 1 mL tube by a magnet (as shown in Figure 1), followed by removing the supernatant and resuspending the magnetic beads in 15 mM MES buffer pH 6.0. Next, 100 μL of EDC was added, and the magnetic beads were incubated on a roller for 30 min. After that, the magnetic beads were washed with 15 mM MES buffer. Subsequently, magnetic beads were incubated with 400 μg of the desired antibodies overnight on a roller. The next day, magnetic beads were washed three times with 0.1 % Tween −20 in PBS. The magnetic beads were resuspended in 0.1 % BSA dissolved in PBS.

Characterization of Modified Reference Electrode. To convert the Ag/AgCl reference electrode's outer surface (surface exposed to liquid) from Ag to AgCl, 1.5 μL of bleach was dripped onto the reference electrode of the SPCE, and the SPCEs were kept in a humidity chamber for 30 min. Following that, SPCEs were washed with 10 mL of DI water. Cyclic voltammetry was performed with 1 mM ferro/ferri cyanide in 1 M KCl (50 μL) from −0.1 to 0.9 V with a 10 mV/s scan rate and 10 mV step size.

Electrochemical Detection of Dissolved AgNPs. AgNPs dissolved in 50 % HNO$_3$ were detected by anodic stripping voltammetry (ASV). Dissolved AgNPs were first deposited on a working electrode by applying −0.5 V for 10 min. After depositing silver onto electrodes, it is stripped from the electrode by a square wave voltammetry scan from −0.5 to 0.5 V (50 mV pulse size, 20 Hz frequency). A peak between 0 and 0.2 V was measured and correlated to Ag concentration.

Immunomagnetic Separation (IMS) with Gold Nanoparticles as an Electrochemical Label. R-antibody modified 1 μm diameter paramagnetic particles (15 μL) along with antigen (500 μL) and Vh-antibody modified 20 nm AuNP (50 μL) were incubated for 1 h on a roller. Next, IMS was used to wash an assay three times with 0.05 % Tween in PBS. Subsequently, an assay was washed three times with 0.05

% Tween in PBS. Finally, an assay was resuspended in 0.1 M HCl in PBS. Part of this solution (60 μL) was used for electrochemical analysis, as described by Patel.[47]

IMS with AgNPs as an Electrochemical Label. R-antibody-modified 1 μm-diameter paramagnetic particles (15 μL) along with antigen (500 μL) and Vh-antibody-modified AgNP (50 μL) were incubated for 1 h on a roller. Next, an assay was washed by replacing the supernatant with 0.05 % Tween in PBS using IMS. Subsequently, an assay was washed three times with 0.05 % Tween in PBS. Finally, 40 μL of HNO$_3$ was incubated in a centrifuge tube for 10 min to dissolve silver nanoparticles, followed by adding 100 μL of electrolyte (0.1 M HNO$_3$ + 0.1 M of NaNO$_3$). Part of this solution (60 μL) was used for electrochemical analysis.

RESULTS

Modified Reference Electrode Potential Measurement. After the SPCEs were modified with bleach, cyclic voltammetry was carried out. The results are shown in Figure 2
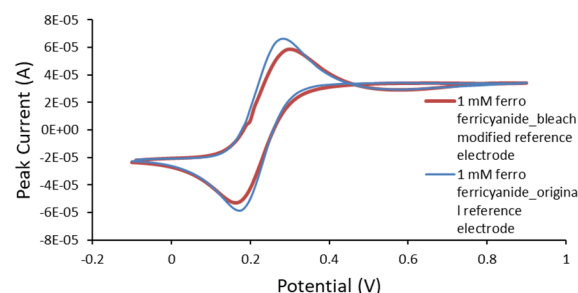

Figure 2. Comparison of regular and bleach-modified reference electrodes of the SPCE by cyclic voltammetry.

and indicate that the reference electrode modified with bleach has the same potential for ferro/ferricyanide (based on peak position in cyclic voltammetry) as the reference electrode without modification. This suggests that silver nanoparticles' electrochemical peak would appear at the exact location and does not need any changes in protocol to deposit or strip silver ions and metal, respectively. Additionally, every SPCE is different, and there is no clear trend of the effect of HNO3 on a signal. However, there were random changes that affected the linearity of the signal and the limit of detection of the signal (data are not shown in the article).

Shiga Toxin-1 Detection Study by AuNPs. To determine the limit of detection of Shiga toxin-1 using the AuNPs-based electrochemical method, the assay with different concentrations of Shiga toxin is performed. However, a high standard deviation in the electrochemical signals was observed, as shown in Figure 3. Hence, a one-way ANOVA followed by an order difference report was generated using a student t-test. This statistical analysis calculates p values between the various experimental pairs blank-1 ng/mL, blank-10 ng/mL, blank-100 ng/mL, and 10 ng/mL-100 ng/mL are calculated as 0.36, 0.0.072, 0.073, and 0.99 respectively. Therefore, 10 and 100 ng/mL are detectable (compared to blank) but not distinguishable. The signal for higher toxin concentration seems to saturate, and evidence of likely hook's effect can also be observed for 1 μg/mL Shiga toxin-1 concentration.[46] Overall, the dynamic range of AuNPs is limited for Shiga toxin-1 detection. The variability in the signal for the AuNp-
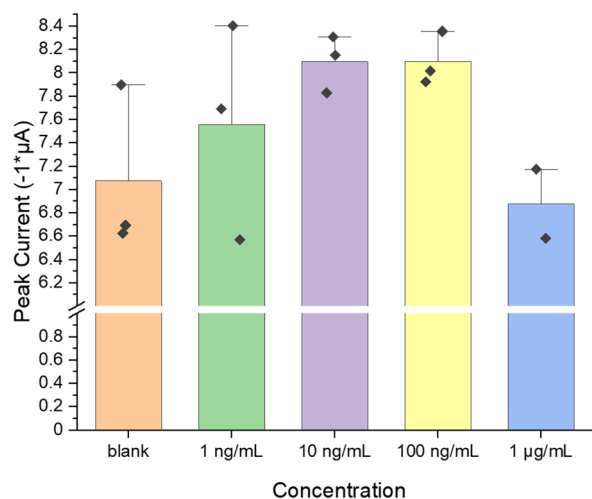
Figure 3. Plot showing the electrochemical detection of Shiga toxin-1 with the AuNP-based assay. (Error bars show standard deviations with three samples for each concentration.)

conjugated toxin likely results from nanoparticle aggregation and incomplete electrochemical dissolution of AuNp.

Shiga Toxin-1 Detection by AgNPs and Detector Response Comparison between AuNPs and AgNPs. To determine the limit of detection of Shiga toxin-1 using the proposed electrochemical method, a series of tests with different concentrations of Shiga toxin is performed. The results presented in Figure 4A indicate that a detection limit of 2 ng/mL Shiga toxin-1 in PBS is possible with a good linear
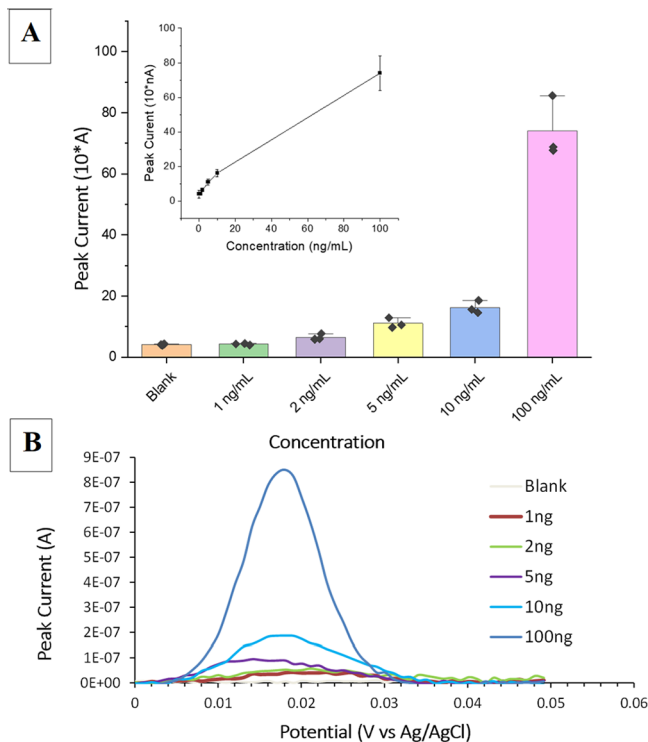

Figure 4. Shiga toxin electrochemical detection: (A) Bar graph of Shiga toxin-1 detection; inset represents a scatter plot of the same graph. (B) Recorded signal of AgNP detections after baseline correction. (Error bars show standard deviations of 3 samples for each concentration.)

relationship between analyte concentration and detector response. It should be noted that this detection limit is within the same order as the manufacturer's Sandwich overnight ELISA's limit of detection. Also, a student *t-test* was run on the blank to 10 ng/mL samples. Based on this statistical analysis, p values between blank-1 ng/mL, blank-2 ng/mL, blank-5 ng/mL, blank-10 ng/mL, and 5 ng/mL-10 ng/mL are calculated as 0.90, 0.043, <0.001, <0.001, and <0.001, respectively. These p values suggest that using AgNPs, 2 ng/mL Shiga toxin-1 detection is possible. Additionally, signals for 2, 5, and 10 ng/mL are distinguishable. Figure 4B shows representative sensograms for the electrochemical detection of Shiga toxin-1 using AgNP as an electrochemical label. Another set of data for Shiga toxin-1, which was run on a different day, is described in the Supporting Information (Figure S2).

By comparing Figures 3 and 4A, we can conclude that AgNP-based detection is statistically better than AuNP-based detection in terms of the detection limit and dynamic range for toxin detection. The reason is that the AuNP-based signal has more variability due to variations in electrochemical dissolution. In contrast, AgNP has more consistent chemical dissolution, leading to less variation and better linear trends for graphs of signal vs concentration. Further dilution buffer exploration could likely improve the detection limit using the same pair of antibodies and AgNPs.

■ DISCUSSION

In this study, we successfully developed an AgNP-based electrochemical detection method for Shiga toxins-1 detection, which is low-cost and faster compared to EIA and PCR with the same order limit of detection. We used low-cost SPCEs and modified their reference electrodes with an in-house process for reliable and repeatable AgNP detection. Despite using low-cost SPCEs, we have achieved the same order detection (2 ng/mL) of Shiga toxin as sandwich-ELISA within 3 h, as described in the certificate of analysis of Shiga toxin antibodies. To our knowledge, no directly comparable electrochemical detection of Shiga toxin-1 exists in the literature. Additionally, a thorough characterization of AgNP electrochemical detection will be done by studying different silver dissolution strategies using different carbon electrodes (different amounts of oxygen groups on the carbon surface) and the effect of AgNP modification on its stability for long-term storage. This assay will be tested with Shiga toxin-contaminated ground beef in future work. Additionally, due to readily available portable batteries and potentiostats, translating this method into a point-of-use diagnostic process with an automated electrochemical flow cell is the next step toward automation.

■ ASSOCIATED CONTENT

⊙ Supporting Information

The Supporting Information is available free of charge at https://pubs.acs.org/doi/10.1021/acsomega.3c06083.

> The Supporting Information includes an experiment to determine the optimal pair of antibodies for detecting Shiga toxin-1 and replicated data of Shiga toxin-1 detection by AgNPs (PDF)

AUTHOR INFORMATION

Corresponding Author

Dhruv Patel − *Department of Mechanical Engineering, University of Utah, Salt Lake City, Utah 84112, United States*; Present Address: 36 S Wasatch Dr #5862, Salt Lake City, Utah 84112, United Sates; orcid.org/0000-0001-8221-3648; Email: U1132490@utah.edu

Authors

Madison Hansen − *Department of Biology, University of Utah, Salt Lake City, Utah 84112, United States*

Christopher Lambert − *Department of Mechanical Engineering, University of Utah, Salt Lake City, Utah 84112, United States; Espira Inc., Salt Lake City, Utah 84103, United States*

Shruti Hegde − *Department of Chemical Engineering, University of Utah, Salt Lake City, Utah 84112, United States*

Harikrishnan Jayamohan − *Department of Mechanical Engineering, University of Utah, Salt Lake City, Utah 84112, United States*

Bruce K. Gale − *Department of Mechanical Engineering, University of Utah, Salt Lake City, Utah 84112, United States; Espira Inc., Salt Lake City, Utah 84103, United States;* orcid.org/0000-0001-5843-3464

Himanshu Jayant Sant − *Department of Mechanical Engineering and Department of Chemical Engineering, University of Utah, Salt Lake City, Utah 84112, United States*

Complete contact information is available at:
https://pubs.acs.org/10.1021/acsomega.3c06083

Notes

The authors declare the following competing financial interest(s): Bruce K. Gale and Himanshu J. Sant have a financial interest in Espira Inc. (Salt Lake City, UT, USA). All conflicts are managed by the University of Utah Conflict of Interest Committee.

ACKNOWLEDGMENTS

We acknowledge the Dr. Marc Porter for sharing his knowledge about electrochemistry.

REFERENCES

(1) Henkel, J. S.; Baldwin, M. R.; Barbieri, J. T. Toxins from Bacteria. *EXS* **2010**, *100*, 1−29, DOI: 10.1007/978-3-7643-8338-1_1.

(2) Todar, K.; *Bacterial Protein Toxins*. [Online]. Available: https://textbookofbacteriology.net/proteintoxins.html.

(3) Rudkin, J. K.; Mcloughlin, R. M.; Preston, A.; Massey, R. C. Bacterial Toxins: Offensive, Defensive, or Something else Altogether? *PLos Pathog.* **2017**, *13* (9), No. e1006452.

(4) Tozzoli, R.; Grande, L.; Michelacci, V.; Maugliani, A.; Caprioli, A.; Morabito, S.; et al. Shiga Toxin-Converting Phages and the Emergence of New Pathogenic Escherichia Coli: A World in Motion. *Front. Cell. Infect. Microbiol.* **2014**, *4*, 80.

(5) Frank, C.; Werber, D.; Cramer, J. P.; Askar, M.; Faber, M.; an der Heiden, M.; Bernard, H.; Fruth, A.; Prager, R.; Spode, A.; Wadl, M.; et al. Epidemic Profile of Shiga-Toxin−Producing Escherichia coli O104:H4 Outbreak in Germany. *N. Engl. J. Med.* **2011**, *365* (19), 1771−1780.

(6) *National Shiga toxin-producing Escherichia coli (STEC) Surveillance Annual Report, 2017*; US Department of Health and Human Services, CDC: Atlanta, GA, 2021.

(7) Frenzen, P. D.; Drake, A.; Angulo, F. J. Economic Cost Of Illness Due To Escherichia Coli O157 Infections In The United States. *J. Food Prot.* **2005**, *68* (12), 2623−2630.

(8) Hoffmann, S.; Maculloch, B.; Batz, M.; *Economic Burden Of Major Foodborne Illnesses Acquired In The United States*, 2015. pp. 1−74.

(9) Riley, L. W.; Remis, R. S.; Helgerson, S. D.; McGee, H. B.; Wells, J. G.; Davis, B. R.; Hebert, R. J.; Olcott, E. S.; Johnson, L. M.; Hargrett, N. T.; Blake, P. A.; et al. Hemorrhagic Colitis Associated With A Rare Escheichia Coli Swrotype. *N. Engl. J. Med.* **1983**, *308* (12), 681−685.

(10) Ashkenazi, S. Role Of Bacterial Cytotoxins In Hemolytic Uremic Syndrome And Thrombotic Thrombocytopenic Purpura. *Annu. Rev. Med.* **1993**, *44* (1), 11−18.

(11) Coia, J. E. Clinical, Microbiological And Epidemiological Aspects Of Escherichia Coli O157 Infection. *FEMS Immunol. Med. Microbiol.* **1998**, *20* (1), 1−9.

(12) Mead, P. S.; Slutsker, L.; Dietz, V.; McCaig, L. F.; Bresee, J. S.; Shapiro, C.; Griffin, P. M.; Tauxe, R. V.; et al. Food-Related Illness And Death In The United States. *J. Environ. Health* **2000**, *62* (7), 9−18.

(13) Wadolkowski, E. A.; Sung, L. M.; Burris, J. A.; Samuel, J. E.; O'brien, A. D. Acute renal tubular necrosis and death of mice orally infected with Escherichia coli strains that produce Shiga-like toxin type II. *Infect. Immun.* **1990**, *58* (12), 3959−3965.

(14) Yutsudo, T.; Takeda, Y.; Honda, T.; Miwatani, T. Physicochemical Characterization of A and B Subunits of Shiga Toxin and Reconstitution of Holotoxin from Isolated Subunits. *Microbiol. Immunol.* **1987**, *31* (3), 189−197.

(15) Eiklid, K.; Olsnes, S. J. U. R. Animal Toxicity Of Shigella Dysenteriae Cytotoxin: Evidence That The Neurotoxic, Enterotoxic, And Cytotoxic Activities Are Due To One Toxin. *J. Immunol.* **1983**, *130* (1), 380−384.

(16) Tesh, V. L.; Burris, J. A.; Owens, J. W.; Gordon, V. M.; Wadolkowski, E. A.; O'brien, A. D.; Samuel, J.; et al. Comparison Of The Relative Toxicities Of Shiga-Like Toxins Type I And Type Ii For Mice. *Infect. Immun.* **1993**, *61* (8), 3392−3402.

(17) Fan, E.; Merritt, E. A.; Verlinde, C. L. M. J.; Hol, W. G. J. Ab5 Toxins: Structures And Inhibitor Design. *Curr. Opin. Struct. Biol.* **2000**, *10* (6), 680−686.

(18) Tam, P. J.; Lingwood, C. A. Membrane-Cytosolic Translocation Of Verotoxin A1 Subunit In Target Cells. *Microbiology* **2007**, *153* (8), 2700−2710.

(19) Hoey, D. E. E.; Sharp, L.; Currie, C.; Lingwood, C. A.; Gally, D. L.; Smith, D. G. E. Verotoxin 1 Binding To Intestinal Crypt Epithelial Cells Results In Localization To Lysosomes And Abrogation Of Toxicity. *Cell. Microbiol.* **2003**, *5* (2), 85−97.

(20) Tam, P.; Mahfoud, R.; Nutikka, A.; Khine, A. A.; Binnington, B.; Paroutis, P.; Lingwood, C.; et al. Differential Intracellular Transport And Binding Of Verotoxin 1 And Verotoxin 2 To Globotriaosylceramide-Containing Lipid Assemblies. *J. Cell. Physiol.* **2008**, *216* (3), 750−763.

(21) Fraser, M. E.; Chernaia, M. M.; Kozlov, Y. V.; James, M. N. Crystal Structure Of The Holotoxin From Shigella Dysenteriae At 2.5 A Resolution. *Nat. Struct. Biol.* **1994**, *1* (1), 59−64.

(22) Fraser, M. E.; Fujinaga, M.; Cherney, M. M.; Melton-Celsa, A. R.; Twiddy, E. M.; O'Brien, A. D.; James, M. N.; et al. Structure of Shiga toxin type 2 (Stx2) from Escherichia coli O157:H7. *J. Biol. Chem.* **2004**, *279* (26), 27511−27517.

(23) Scheutz, F.; Beutin, L.; Piérard, D.; Buvens, G.; Karch, H.; Mellmann, A.; Caprioli, A.; Tozzoli, R.; Morabito, S.; Strockbine, N. A.; et al. Multicenter Evaluation Of A Sequence-Based Protocol For Subtyping Shiga Toxins And Standardizing Stx Nomenclature. *J. Clin. Microbiol.* **2012**, *50* (9), 2951−2963.

(24) Tarr, P. I.; Gordon, C. A.; Chandler, W. L. Shiga-Toxin-Producing Escherichia Coli And Haemolytic Uraemic Syndrome. *Lancet* **2005**, *365* (9464), 1073−1086.

(25) Fuller, C. A.; Pellino, C. A.; Flagler, M. J.; Strasser, J. E.; Weiss, A. A. Shiga Toxin Subtypes Display Dramatic Differences In Potency. *Infect. Immun.* **2011**, *79* (3), 1329−1337.

(26) Melton-celsa, A. R. Shiga Toxin (Stx) Classification, Structure, and Function. *Microbiol. Spectr.* **2014**, *2* (4), 2.

(27) Trachtman, H.; Austin, C.; Lewinski, M.; Stahl, R. A. K. Renal And Neurological Involvement In Typical Shiga Toxin-Associated HUS. *Nat. Rev. Nephrol.* **2012**, *8* (11), 658−669.

(28) Kimmitt, P. T.; Harwood, C. R.; Barer, M. R. Toxin Gene Expression By Shiga Toxin-Producing Escherichia Coli: The Role Of Antibiotics And The Bacterial Sos Response. *Emerg. Infect. Dis.* **2000**, *6* (5), 458−465.

(29) Al-qarawi, S.; Fontaine, R. E.; Al-qahtani, M. S. An Outbreak Of Hemolytic Uremic Syndrome Associated With Antibiotic Treatment Of Hospital Inpatients For Dysentery. *Emerg. Infect. Dis.* **1995**, *1* (4), 138−140.

(30) Walterspiel, J. N.; Ashkenazi, S.; Morrow, A. L.; Cleary, T. G. Effect Of Subinhibitory Concentrations Of Antibiotics On Extracellular Shiga-Like Toxin I. *Infection* **1992**, *20* (1), 25−29.

(31) Gould, L. H.; STEC Clinical Laboratory Diagnostics Working Group. Recommendations for Diagnosis of Shiga Toxin--Producing Escherichia coli Infections by Clinical Laboratories; Division of Foodborne, Bacterial, and Mycotic Diseases, National Center for Zoonotic, Vector-Borne, and Enteric Diseases, CDC, 2009. [Online]. Available: https://www.cdc.gov/mmwr/preview/mmwrhtml/rr5812a1.htm#:~:text=Recently%2C.

(32) Huang, L.; Chen, J.; Yu, Z.; Tang, D. Self-Powered Temperature Sensor with Seebeck Effect Transduction for Photothermal−Thermoelectric Coupled Immunoassay. *Anal. Chem.* **2020**, *92* (3), 2809−2814.

(33) Singh, A.; Sharma, A.; Ahmed, A.; Sundramoorthy, A. K.; Furukawa, H.; Arya, S.; Khosla, A.; et al. Recent advances in electrochemical biosensors: applications, challenges, and future scope. *Biosensors* **2021**, *11* (9), 336.

(34) Mehrvar, M.; Abdi, M. Recent Developments, Characteristics, And Potential Applications Of Electrochemical Biosensors. *Anal. Sci.* **2004**, *20* (8), 1113−1126.

(35) Kaya, H. O.; Cetin, A. E.; Azimzadeh, M.; Topkaya, S. N. Pathogen Detection With Electrochemical Biosensors: Advantages, Challenges And Future Perspectives. *J. Electroanal. Chem.* **2021**, *882*, No. 114989.

(36) Lin, Y.; Zhou, Q.; Tang, D.; Niessner, R.; Yang, H.; Knopp, D. Silver Nanolabels-Assisted Ion-Exchange Reaction with CdTe Quantum Dots Mediated Exciton Trapping for Signal-On Photoelectrochemical Immunoassay of Mycotoxins. *Anal. Chem.* **2016**, *88* (15), 7858−7866.

(37) Zhu, L.; Yin, Z.; Lv, Z.; Li, M.; Tang, D. Ultrasensitive photoelectrochemical immunoassay for prostate-specific antigen based on silver nanoparticle-triggered ion-exchange reaction with ZnO/CdS nanorods. *Analyst* **2021**, *146* (14), 4487−4494.

(38) Filbrun, S. L. *Formation, Characterization, And Optimization Of Antibody-Gold Nanoparticle Conjugates*; Illinois State Univ., 2017.

(39) Zhang, L.; Mazouzi, Y.; Salmain, M.; Liedberg, B.; Boujday, S. Antibody-Gold Nanoparticle Bioconjugates for Biosensors: Synthesis, Characterization and Selected Applications. *Biosens. Bioelectron.* **2020**, *165*, No. 112370.

(40) Okyem, S.; Awotunde, O.; Ogunlusi, T.; Riley, M. B.; Driskell, J. D. High-Affinity Points of Interaction on Antibody Allow Synthesis of Stable and Highly Functional Antibody-Gold Nanoparticle Conjugates. *Bioconjug. Chem.* **2021**, *32* (8), 1753−1762.

(41) Austin, L. A.; Mackey, M. A.; Dreaden, E. C.; El-sayed, M. A. The Optical, Photothermal, And Facile Surface Chemical Properties Of Gold And Silver Nanoparticles In Biodiagnostics, Therapy, And Drug Delivery. *Arch. Toxicol.* **2014**, *88* (7), 1391−1417.

(42) López-Millán, A.; Zavala-Rivera, P.; Esquivel, R.; Carrillo, R.; Alvarez-Ramos, E.; Moreno-Corral, R.; Guzmán-Zamudio, R.; Lucero-Acuña, A. Aqueous-Organic Phase Transfer Of Gold And Silver Nanoparticles Using Thiol-Modified Oleic Acid. *Appl. Sci.* **2017**, *7* (3), 273 DOI: 10.3390/app7030273.

(43) ″Gold, Silver, Platinum and Palladium Live Spot Prices,″ Money Metals. [Online]. Available: https://www.moneymetals.com/precious-metals-charts.

(44) Maccuspie, R. I. Colloidal Stability Of Silver Nanoparticles In Biologically Relevant Conditions. *J. Nanoparticle Res.* **2011**, *13* (7), 2893−2908.

(45) Pinto, V. V.; Ferreira, M. J.; Silva, R.; Santos, H. A.; Silva, F.; Pereira, C. M. Long Time Effect On The Stability Of Silver Nanoparticles In Aqueous Medium: Effect Of The Synthesis And Storage Conditions. *Colloids Surf. A Physicochem. Eng. Asp.* **2010**, *364* (1), 19−25.

(46) Jacobs, J. F. M.; Van der molen, R. G.; Bossuyt, X.; Damoiseaux, J. Antigen excess in modern immunoassays: To anticipate on the unexpected. *Autoimmun. Rev.* **2015**, *14* (2), 160−167.

(47) Patel, D.; Jayamohan, H.; Nze, U.; Lambert, C.; Feng, H.; Mahmood, T.; Gale, B.; Sant, H.; et al. Design Of A Hydrodynamic Cavitation System For The Extraction And Detection Of Escherichia Coli (O157: H7) From Ground Beef. *Sens. Actuators B Chem.* **2022**, *369*, No. 132370.

(48) Dynabeads MyOne Carboxylic Acid. Available online: https://www.thermofisher.com/document-conect/docment-connect.html?url=https://assets.thermofisher.com/TFS-ssets%2FLSG%2Fmanuals%2F65011_65012_Dynabeads_MyOne_Carboxylic_Acid_PI.pdf (accessed on 17 April 2023).